analytical chemistry

Article

Cite This: Anal. Chem. 2018, 90, 752−759

pubs.acs.org/ac

Online Differential Thermal Isotope Analysis of Hydration Water in Minerals by Cavity Ringdown Laser Spectroscopy

T. K. Bauska,* G. Walters, F. Gázquez, and D. A. Hodell

Godwin Laboratory for Palaeoclimate Research, Department of Earth Sciences, University of Cambridge, Downing Street, Cambridge CB2 3EQ, United Kingdom

ABSTRACT: We have developed a new method for measuring the isotopic composition ($\delta^{18}O$ and δD) of different types of bonded water (e.g., molecular water, hydroxyl) contained in hydrated minerals by coupling a thermal gravimeter (TG) and a cavity ringdown laser spectrometer (CRDS). The method involves precisely step-heating a mineral sample, allowing the separation of the different types of waters that are released at different temperatures. Simultaneously, the water vapor evolved from the mineral sample is analyzed for oxygen and hydrogen isotopes by CRDS. Isotopic values for the separate peaks are calculated by integrating the product of the water amounts and its isotopic values, after correcting for background. We provide examples of the application of the differential thermal isotope analysis (DTIA) method to a variety of hydrous minerals and mineraloids including gypsum, clays, and amorphous silica (opal). The isotopic compositions of the total water evolved from a set of natural gypsum samples by DTIA are compared with the results of a conventional offline water extraction method followed by CRDS analysis. The results from both methods are in excellent agreement, and precisions (1σ) for $\delta^{18}O$ ($\pm 0.12‰$) and δD ($\pm 0.8‰$) of the total gypsum hydration water from the DTIA method are comparable to that obtained by the offline method. A range of analytical challenges and solutions (e.g., spectroscopic interferences produced by VOCs in natural samples, isotopic exchange with structural oxygen, etc.) are discussed. The DTIA method has wide ranging applications for addressing fundamental problems across many disciplines in earth and planetary sciences, including paleoclimatology, sedimentology, volcanology, water exchange between the solid earth and hydrosphere, and water on Mars and other planetary bodies.

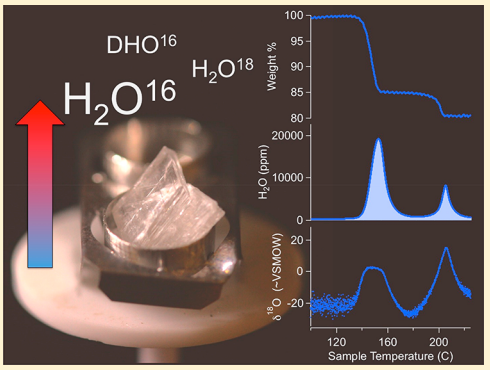

Oxygen (^{16}O,^{17}O,^{18}O) and hydrogen (H,D) isotopes of hydration water in minerals provide powerful constraints on the conditions under which these minerals form on Earth and other planetary bodies (e.g., Mars). High-precision measurements of hydrated minerals present three major challenges: (i) hydrated minerals often hold multiple forms of water of variable exchangeability and isotopic composition that require separation prior to analysis; (ii) most natural samples are of mixed mineralogy that are not readily separable by mechanical or chemical means; and (iii) oxygen and hydrogen need to be converted to, or in equilibration with, gaseous species for analysis on gas-source isotope ratio mass spectrometer (typically CO_2 for $\delta^{18}O$, O_2 for ^{17}O-excess, H_2 for δD). Here we outline a new method that couples a thermal gravimeter to a cavity ringdown laser spectrometer, thus allowing for precise thermal separation and simultaneous online analysis that bypasses the need for chemical conversion. We refer to the method as "on-line differential thermal isotope analysis" (online DTIA). General methodology is described with a focus on gypsum, a relatively well-studied hydrated mineral, in order to provide information on protocol, data processing requirements, accuracy, and precision. Other mineral examples including kaolinite, montmorillonite, and opal are used to describe some specific advantages and limitations of the method.

Research on the isotopic composition of hydrous minerals progressed rapidly in the 1960s and 1970s following the advent of gas-source isotope ratio mass spectrometry (IRMS). Pioneering work was carried out on volcanic glass,[1] gypsum,[2] opal,[3] clays,[4−9] hydrous carbonates,[10] and manganese hydroxides.[11] Typically, water was extracted by heating in vacuum followed by cryogenic trapping and finally conversion to, or exchange with, H_2 or CO_2 gas (though most early studies focused solely on hydrogen isotopes). In order to separate different types of water within a given mineral, Knauth and Epstein, in 1982, developed a method whereby a mineral (opal in particular) was progressively heated in vacuum and water was trapped over discrete temperature intervals for later analysis by IRMS.[12] A quartz spring balance within the vacuum system allowed the authors to monitor the mass loss over the course of the experiment. The method was termed "differential thermal isotope analysis" and has subsequently been adopted for a variety of hydrous mineral studies. The downsides to the method include the laborious nature of the trapping procedure (a typical experiment lasted over 8 h) and the need for chemical conversion of the water to H_2 or CO_2 gas.

Received: August 4, 2017
Accepted: November 13, 2017
Published: November 13, 2017

DOI: 10.1021/acs.analchem.7b03136
Anal. Chem. 2018, 90, 752−759

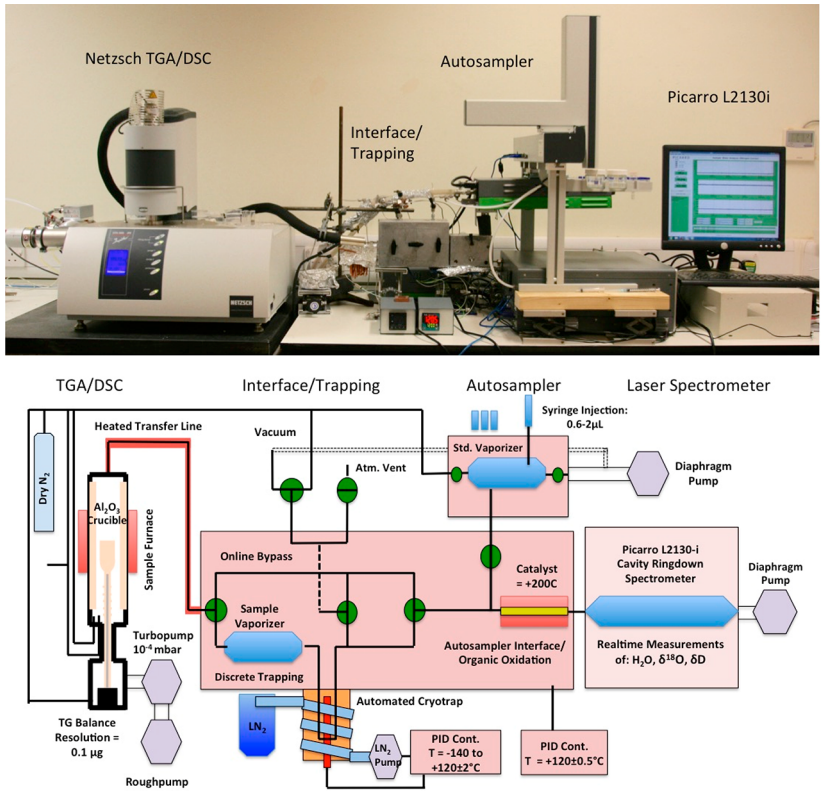

Figure 1. Online-DTIA system overview. Upper panel: An image of the coupled Netzsch thermal gravimetric analysis (TGA) unit and Picarro L2130i cavity ringdown spectrometer (CRDS). Lower panel: A schematic of the system with an emphasis on the interface box. Solid black lines represent 1/8 in. stainless steel tubing, and green circles represent valves.

In the 1990s and early 2000s, methods became available for online extraction of water and rapid conversion to gaseous species suitable for continuous-flow mass spectrometry[13,14] Using a high-temperature (1450°C) glassy carbon furnace to simultaneously dehydrate/dehyroxylate minerals and convert H_2O vapor to H_2 and CO gas, Sharp et al., in 2001, demonstrated high-precision measurements of δD of ±2‰ (1σ) on a variety of hydrous minerals on samples containing about 0.1 μL of H_2O.[14] The method also showed promise for the simultaneous analysis of $\delta^{18}O$ (by peak-jumping the IRMS to CO m/z) with precisions of 0.2‰ (1σ), but this aspect of the method has been less widely reported in the literature. Any differential thermal isotope analysis with this method requires preheating the samples to remove unwanted water followed by methods to prevent any absorption of atmospheric water vapor prior to analysis. More specialized systems have also been developed to study the hydrogen isotopes of nominally nonhydrous geologic samples (e.g., meteorites) with precisions ranging from ±1 to 2‰ (1σ) on samples yielding as little as 1 × 10^{-5} μL of H_2O.[15]

More recently, the development of commercially available laser absorption spectrometers has offered another opportunity for technical advancement. Offline extraction of gypsum hydration water followed by CRDS analysis (Picarro i2140) has yielded high-precision measurements of $\delta^{18}O$, $\delta^{17}O$, and δD with 1σ standard deviations of 0.13‰, 0.07‰, and 0.5‰, respectively, for water samples of about 40 μL (200 mgs of gypsum).[16] CRDS instruments have also been used in the measurements of much smaller amounts of water released from fluid inclusions in minerals (~0.1−1.0 μL) with precision better than ~0.5‰ and 2‰ (1σ) for $\delta^{18}O$ and δD, respectively.[17−19] An online method using off-axis integrated cavity output spectroscopy (Los Gatos Research model 908-004), which focused on organic materials but reported some gypsum measurements, demonstrated precisions of ±3−4‰ (1σ) for δD.[20] Here we take advantage of this recent advance in laser spectroscopy and revisit the "differential thermal isotope analysis" method described by Knauth and Epstein[12] with state-of-the-art instrumentation.

SYSTEM DESIGN

An overview schematic of the online-DTIA system is provided in Figure 1. Samples are heated in a thermal analysis system (Netzsch STA 449 F3 Jupiter) capable of both thermal gravimetric analysis (TGA) and differential scanning calorimetry (DSC). The furnace can range between ambient temperature and 1600° C with maximum ramp rates of 40 °C/min and the possibility of precisely controlled plateaus. TGA provides continuous data on changes in the mass of the sample with time and temperature. DSC records small differences in the temperature of the sample and a reference material, thus providing constraints on the enthalpy of a phase transition or chemical reaction (i.e., endothermic or exothermic). TGA and DSC are standard analytical techniques in earth sciences that use characteristic thermal reactions for rapid and inexpensive mineral identification.[21]

A sample is held in a crucible that sits perched on a "carrier" that connects to the balance, which is composed of an alumina stalk housing the thermocouple and alumina baffle system. For samples smaller than ~20 mg, we typically use a TGA/DSC carrier, which has a platinum platform that can hold a variety of crucibles (Al for temperatures less than 600 °C, Pt or Al_2O_3 for

DOI: 10.1021/acs.analchem.7b03136
Anal. Chem. 2018, 90, 752−759

higher temperatures). Larger samples (up to 5 mL in volume) are analyzed solely in TGA mode and are held in an Al_2O_3 crucible that fits directly onto the carrier stalk.

The flow of gas can be precisely manipulated by controllers in the TG system to broadly match the flow required by the Picarro instrument, (~30 mL/min), although in practice we found that variability in the flow rate of the Picarro on the order of hours to days can lead to slight over- and underpressures within the balance system. Underpressures are not problematic as the TG system is designed to operate with pressure as low as 10^{-4} mBar (with an attached turbmolecular pumping system not used in this study), but large overpressures can potentially damage the balance. We employ an open-split upstream of the TGA in the gas flow to prevent overpressures. Generally, we use dry N_2 as a carrier gas although some experiments require the use of dry air (or an N_2/O_2 mixture) as a source of O_2 when a catalyst is employed to oxidize organic molecules (see below). Stock o-rings on many of the seals in the TG system, likely of silicone and relatively permeable to water, were replaced with Viton.

Downstream of the TGA, water vapor is carried via a heated (120°C) 1/8 in. stainless steel tube to a heated (120 °C) interface system. The purpose of the interface box is 3-fold: to switch between the autosampler and Netzsch without disrupting the gas flow to either instrument; to house a cryogenic trapping system; and to provide an optional catalyst for removal of impurities (e.g., VOCs) in the gas flow. The gas plumbing is composed primarily of 1/8 in. stainless steel tubing and Swagelok 3-way ball valves (40G series). The vaporizer reservoir is a 50 cm^3 stainless steel cylinder (Swagekok part no. SS-4CD-TW-50). A "U" trap of 1/4 in. stainless steel tubing sits outside the box, jacketed in solid copper, and heated with a PID controlled cartridge heater to 120 °C. In trapping mode, the PID is set to −70 °C, and the copper jacket is cooled by direct contact with liquid nitrogen. When a catalyst is required, a 1/4 in. stainless steel tube containing a rare earth catalyst and heated to over 200 °C is inserted immediately upstream of the CRDS instrument (and downstream of the autosampler junction). The catalyst material is sourced from an off-the-shelf catalytic converter, which has proven to be as effective and cost-efficient.

A Picarro L-2130i provides continuous measurement of the H_2O, $\delta^{18}O$, and δD of the water vapor stream. No significant modifications of the analyzer were required although we found it is important to analyze parameters such as the "baseline shift" and "residual" to monitor for contamination.

ANALYTICAL PROTOCOL

A sample is loaded into the TGA system manually, and the furnace tube is flushed with N_2 (30 mL/min) for at least 15 min or until water background returns to less than 100 ppm. A temperature program is then started, and the TGA and Picarro water isotopes traces are synchronized. Figure 2 shows an example of a gypsum dehydration profile with the coupled TGA/DSC and Picarro data traces. In this case, gypsum was placed in loosely sealed aluminum crucible to produce the two-step dehydration from gypsum ($CaSO_4{\cdot}2H_2O$) to bassananite ($CaSO_4{\cdot}0.5H_2O$) to anhydrite ($CaSO_4$), which illustrates the ability of the system to separate different bonded waters and simultaneous characterize them for their mass loss, enthalpy, H_2O, $\delta^{18}O$, and δD. As the sample is heated (5 °C min^{-1}), the mineral dehydrates as evidenced by the mass loss and endothermic reaction. The released water vapor is carried to

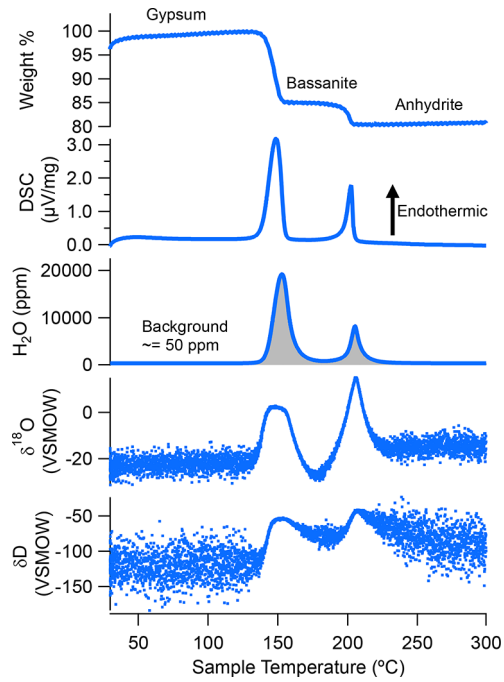

Figure 2. An example of a gypsum−bassanite−anhydrite transition with the well-known double release of structural water. The weight % and differential scanning calorimety (DSC) traces from the Netzsch TGA/DSC are shown in the upper two panels. The lower panels show the H_2O, $\delta^{18}O$, and δD traces from the Picarro CRDS.

the CRDS (transit time ~<1 min) where it is measured for H_2O concentration, $\delta^{18}O$, and δD. After analysis, the furnace is cooled to near ambient temperature, and another sample may be loaded immediately. Samples like gypsum, which require relatively low final temperatures (~200 °C), can be measured about every 40 min. Samples requiring higher final temperatures (~1000 °C) require at least a 90 min turn-around period.

DATA PROCESSING

Raw data output from the TGA/DSC and Picarro instruments are processed with in-house Matlab code. Peak shoulders are defined on the basis of the first derivate of the H_2O trace. Background levels of H_2O and the isotopic values before and after the peak are determined by a linear fit between the two intervals that is assumed to represent the background H_2O, $\delta^{18}O$, and δD across the sample peak. Typically, background in the instrument is low (~50 ppm) relative to an ideal sample peak height of ~18 000 ppm. The background in the instrument is sourced from lab air with some memory effects from prior samples with $\delta^{18}O$ and δD values of around −20‰ and −140‰, respectively. The magnitude of the correction thus varies depending on both the sample amount and isotopic composition. We treat this as a a preliminary correction that should be evaluated on a case-by-case basis using a suite of known isotopic standards of varying sample amounts (see section on Accuracy). Total H_2O, $\delta^{18}O$, and δD are calculated by integrating the H_2O, $\delta^{18}O$, and δD traces and correcting them for background. Background corrected values for $\delta^{18}O$ and δD are then calibrated using at least three working water standards (calibrated against SLAP, GISP, and V-SMOW) that are injected multiple times into a vaporizer following the approach outlined in Gazquez et al., in 2015.[16]

DOI: 10.1021/acs.analchem.7b03136
Anal. Chem. 2018, 90, 752−759

GYPSUM RESULTS: PRECISION, ACCURACY, AND LINEARITY

We use gypsum as a means to characterize the precision, accuracy, and sensitivity of the online-DTIA method. First, we measured a suite of natural and synthetic gypsum samples with a wide range of isotopic values with both the online-DTIA method and an offline, in vacuum total hydration water extraction system (the "WASP").[16,22] The WASP system requires sample amounts of around 200 mg of gypsum, yielding 40 μL of water or enough to allow 10 syringe injections of 2 μL each into the CRDS. We then measured the same samples with the online-DTIA method. In comparison, the online-DTIA method consumes only ~7 mg of sample, thus yielding ~1.4 μL of water. The results of the comparison are shown in Figure 3 where the total gypsum hydration water

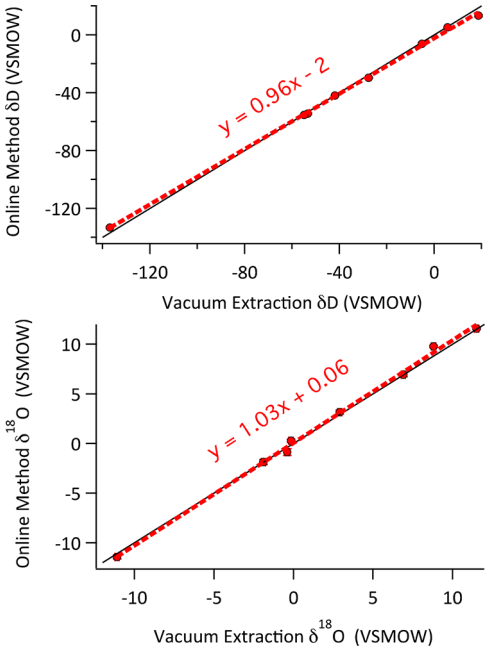

Figure 3. Gypsum precision and accuracy. Plots of total gypsum hydration water δ^{18}O and δD in natural and synthetic samples gypsum from a high-precision, offline vacuum extraction technique (Gazquez et al., 2015) and the online-DTIA technique (this study). The black solid lines represent the 1:1 line of coincidence between the two methods.

δ^{18}O and δD from the "WASP" method are plotted against the results from the online-DTIA method. In the δ^{18}O comparison, a linear regression yielded a slope, intercept, and root-mean-square error of 1.03, 0.06, and 0.35‰, respectively; the δD comparison produces a slope, intercept and root-mean-square error values of 0.96, −2.41, and 1.3‰, respectively. The comparison demonstrates that, with a reduction in sample size of over an order of magnitude, the online-DTIA method can accurately determine the isotopic composition of GHW across a wide range of values to within about 0.4‰ and 1.3‰ for δ^{18}O and δD, respectively.

In the online-DTIA method there is always a trade-off between the sample peak height and width. For a given sample size faster heating ramps will produce higher but narrower peaks, whereas slower heating ramps will produce lower but broader peaks. Although instrumental response of the Picarro is considered to be relatively linear and precise down to 2500 ppm (quoted precision at 2500 ppm of 0.08‰ for δ^{18}O and 0.50‰ for δD over a 100 s integration time in the Picarro gray literature), it has been shown that this should be evaluated on a case-by-case basis.[23,24] In the online-DTIA, other effects could include the contributions from the background, any additional absorbed water on the surface of the furnace tube, and any nonlinear response of the measured δ^{18}O and δD to changing water vapor concentration, particularly across the "shoulders" of the peak when H_2O is less than 2500 ppm. To characterize these potential effects we made repeated measurements of one homogeneous gypsum sample of known isotope composition across a range of sample sizes and heating ramp rates. This allows us to characterize the reproducibility and measurement linearity across a range of total water extracted and peak height. The results, plotted against total water released (0.09−2.4 μL) and broken down by heating ramp rate (5−40 °C per minute) are shown in Figure 4.

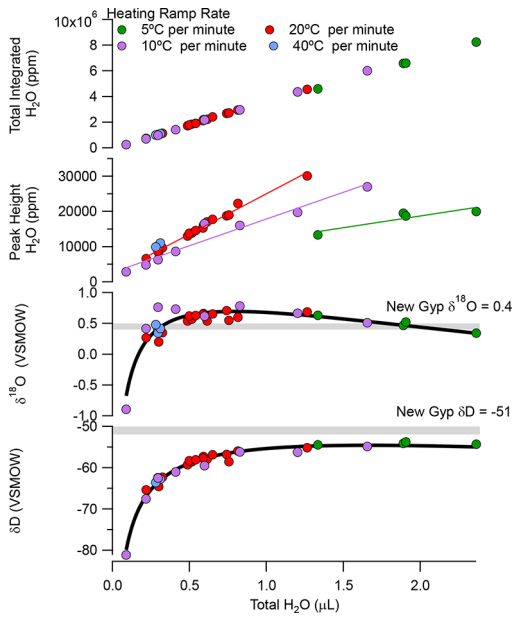

Figure 4. Gypsum δ^{18}O and δD sample size dependence. Plots of total integrated water, peak height, and the precision and accuracy of δ^{18}O and δD from an internal gypsum standard "NEWGYP" (δ^{18}O = 0.45‰; δD = −51‰, indicated by horizontal gray bars). Experiments were carried out with variable sample sizes and heating ramp rates to quantify their effect on precision and accuracy. The gray shades represent the mean values (±1σ) of the same standard obtained by the offline extraction followed by CRDS analysis (Gazquez et al., 2015).[16]

The measured δ^{18}O and δD values are relatively stable above 1 μL with means and 1σ standard deviations of 0.58 ± 0.12‰ and −54.9 ± 0.8‰, respectively. Between 0.5 and 1 μL, δ^{18}O remains stable (0.63 ± 0.07‰) but δD begins to systematic trend toward negative values (−57.6 ± 1.1‰). Between 0.2 and 0.5 μL, δ^{18}O becomes noisier (0.46 ± 0.18‰), and δD falls precipitously toward negative values (−62.7 ± 2.5‰). One sample below 0.1 μL is very depleted. Trends in error (both random and systematic) appear to correlate most strongly with sample size amount and are relatively insensitive to peak height between 5000 and 30 000 ppm, suggesting the method is limited by sample size amount. The most robust data will come from samples yielding above 1.0 μL of H_2O with ramp rates that produce peak heights of 10 000−20 000 ppm. Within this range, the 1σ standard deviations for δ^{18}O and δD are ±0.12‰

DOI: 10.1021/acs.analchem.7b03136
Anal. Chem. 2018, 90, 752−759

and ±0.8‰, respectively. Samples yielding between 0.2 and 1.0 μL should be run alongside known standards to account for systematic errors.

KAOLONITE AND MONTMORILLONITE: HIGH-TEMPERATURE DEHYDROXYLATION EXAMPLES

In addition to providing precise and routine isotopic measurements on relatively small samples, a significant innovation of the system is the capability of separating different types of bonded water. Here we report preliminary measurements of the isotopic composition of samples of kaolinite (source: Blackpool Pit, St. Austell pluton, Cornwall, UK[25]) and montmorillonite (source: Clay Minerals Society Stx-1b). Kaolinite, $Al_2Si_2O_5(OH)_4$, is a simple clay with only bonded hydroxyl, thus allowing us to compare the online-DTIA method to an offline technique. Montmorillonite, $(Na,Ca)_{0.33}(Al,Mg)_2(Si_4O_{10})(OH)_2{\cdot}nH_2O$, is a clay with both interlayer water and bonded hydroxyl, a more representative example of water found in phyllosilicates. Examples of the weight %, H_2O, $\delta^{18}O$, and δD traces are shown in Figure 5.

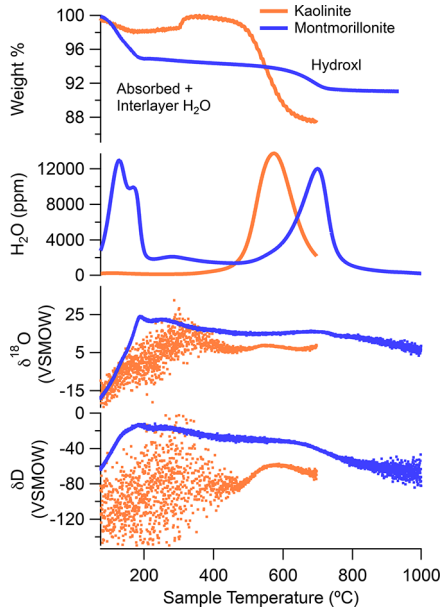

Figure 5. Kaolinite and montmorillonite examples. A comparison of the kaolinite (orange) dehydroxylation centered around 450 °C and the montmorillonite interlayer and absorbed water dehydration around 150 °C and dehydroxylation which peaks around 600 °C.

Kaolinite undergoes dehydroxylation from ∼450 to 650 °C, producing a relatively symmetric peak in H_2O (note the mass increase at 300 °C is an uncorrected artifact from an increase in the temperature ramp rate). On the basis of four replicate measurements with the online-DTIA system, the $\delta^{18}O$ and δD of the hydroxyl water are +6.63 ± 0.7‰ and −62.2 ± 0.7‰, respectively. These results agree, within error, with those offline in vacuum extractions (n = 5) of significantly larger samples in our laboratory ($\delta^{18}O$ = +5.8 ± 0.5‰ and δD = −62.6 ± 3.7‰) and δD determined by early offline extraction and gas-source mass spectrometry techniques (δD = −62‰).[25] This demonstrates that water extraction at high temperature with the online-DTIA method is free of any significant errors with respect to previously established methodologies.

Montmorillonite shows a highly convolved double peak from ∼100 to 200 °C from interlayer and absorbed water with both $\delta^{18}O$ and δD trending toward enriched values. From 200 to 500 °C, the sample continues to slowly lose mass (∼0.003 wt %/°C). This leads to elevated water vapor levels between 2000 and 3000 ppm. Dehydroxylation appears to begin around 500 °C with a significant acceleration of water loss between 600 and 700 °C. In cases like this, an isothermal interval can be employed to increase separation between peaks. Using this technique (not shown), replicate measurements (n = 4) constrain the $\delta^{18}O$ and δD of the hydroxyl peak to +13.42 ± 0.13‰ and −41.6 ± 0.6‰, respectively. This demonstrates the possibility for high-precision measurements of clay minerals. Attempts to separate and measure the hydroxyl water with offline extraction proved unsuccessful, highlighting the utility of the online-DTIA method but limiting our ability to access the accuracy of the online-DTIA method.

HYDRATION WATER IN OPAL: CONTAMINATION FROM ORGANICS AND CARBONATE

Opal is an example of a hydrated mineral with a large amount of absorbed and/or loosely bonded H_2O (∼>5 wt %) relative to hydroxyl (<1%). Moreover, the H_2O and OH peaks are highly convolved. Nonetheless, opal is an attractive mineral to study given its widespread occurrence in the geologic record. During the course of experimentation with natural samples (primarily diatomaceous oozes from deep ocean cores and terrestrial diatomites), we have identified three possible limitations of the online-DTIA method that require evaluation on a case-by-case basis.

Volatilized organic molecules can interfere with the infrared spectra of water isotopes when using CRDS, leading to erroneous isotopic data that is typically too enriched.[26] Organic carbon pyrolysis and subsequent spectral interference can be monitored by a close comparison of the mass loss (from the TGA), cumulative H_2O released (from the CRDS), and CRDS parameters for spectral contamination (baseline shift, baseline curvature, residual, CH_4). Intervals of mass loss without a corresponding release of H_2O can be flagged as potentially contaminated and discarded. To illustrate this a comparison of a raw opal sample and a sample cleaned with H_2O_2 is shown in Figure 6. In the raw sample, excess mass loss in the contaminated sample of about 1 wt % is observed from 450 to 500 °C. Simultaneous increases in the spectral "residual" (or baseline shift, not shown) and fluctuations in the $\delta^{18}O$ trace point toward problematic contamination. Additional measures can be taken to mitigate the effect of organic contamination through the use of an air carrier gas in conjunction with a rare earth catalyst to promote the oxidization of organic molecules to CO_2 and H_2O.[16] Future work could explore using laser spectrometers that utilize significantly different wavelengths than the Picarro CRDS and thus avoid this potentially problematic contamination.

Many natural geologic samples contain carbonate minerals and thus undergo calcination above about 700 °C (reaction: $CaCO_3 \rightarrow CaO + CO_2$). Nascent CO_2 and H_2O released at high temperature is capable of rapid oxygen isotope exchange,[27] although the two gas species likely need a surface or catalyst to promote the reaction. Given that the oxygen isotope fractionation during the conversion of $CaCO_3$ to CO_2[28] and exchange between CO_2 and H_2O[29] are small at high temperature, an observed $\delta^{18}O$–H_2O trace subject to exchange with CO_2 sourced from carbonate will broadly approach the

DOI: 10.1021/acs.analchem.7b03136
Anal. Chem. 2018, 90, 752−759

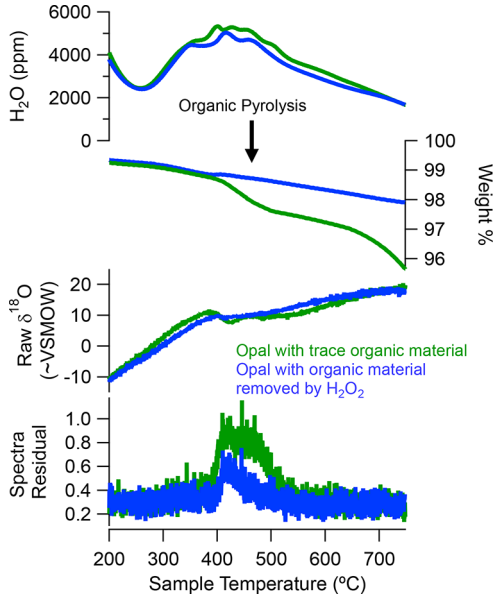

Figure 6. Organic contamination in biogenic silica samples. An example of an opal sample dehydroxylation when organic matter contamination undergoes pyrolysis (green lines). Organic content of this sample is about 1 wt % as shown with the additional around 450 °C without any corresponding increase in H_2O. For comparison, the same sample was treated with H_2O_2 to remove organic matter prior to heating (blue). Note the increase in the spectrum residual during pyrolysis that can act as a flag for contamination.

isotopic composition of carbonate substrate. With most terrestrial carbonates enriched in ^{18}O, on the order of ~ +30‰ VSMOW, the $\delta^{18}O-H_2O$ trace will typically erroneously climb toward enriched values during calcination. Figure 7 shows an example of terrestrial diatomite containing trace

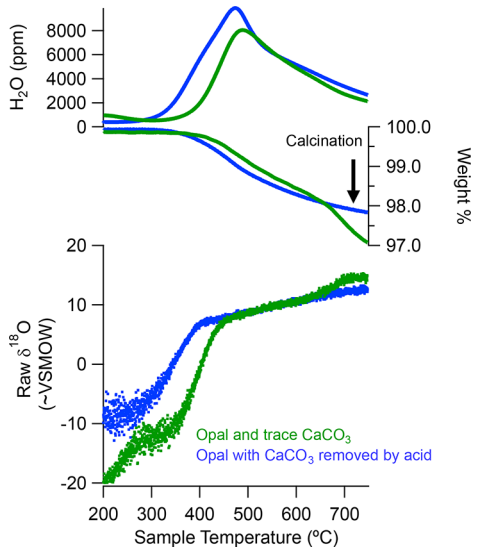

Figure 7. Carbonate contamination. Examples of opal dehydroxylation both with (green) and without (blue) the presence of trace $CaCO_3$. One opal sample contained at least 1 wt % $CaCO_3$ as noted by the additional anomalous mass loss above about 700 °C. This carbonate would be very enriched in $\delta^{18}O$ (+30‰, VSMOW) and would produce CO_2 gas upon calcination. The anomalous increase in $\delta^{18}O$ of the contaminated sample above about 700 °C is attributed to exchange between the nascent H_2O and CO_2.

amount of $CaCO_3$ (~1 wt %) both before and after acidification with HCl. Calcination around 700 °C leads to enrichments of +2−3‰. When possible, samples should be treated with weak acid to remove carbonates, but tests with isotopically spiked acid solutions must be carried to check for the possibility of isotopic exchange during acidification.

Future work to quantify the amount and isotopic composition of CO_2 produced from calcination could be made by incorporating a CO_2 isotope CRDS downstream of the H_2O isotope CRDS or using a combined CO_2 and H_2O isotope analyzer.[30] Simultaneous measurement could provide the means to constrain the isotopic exchangeability of CO_2 and H_2O during an experiment. Additionally, continuous measurement of the concentration and isotopes of CO_2 produced at high temperature from carbonate minerals would allow a re-evaluation of the thermal decarbonization method as a means for measuring the isotopic composition of carbonate minerals.[31,32]

POTENTIAL FOR OXYGEN ISOTOPE EXCHANGE AT HIGH TEMPERATURE

The oxygen isotopic composition of the hydrous components of minerals is less-frequently studied and reported compared to the hydrogen isotopic composition. This is in part due to concerns about oxygen isotopic exchange between the hydrous and nonhydrous oxygen during high-temperature dehydroxylation. In the case of opal, we observed clear evidence that a sample can undergo isotopic exchange between water vapor and nonhydrous oxygen upon heating. Tests with other minerals are underway but do not provide such clear evidence, and as such, opal may be a particular case owing to the amorphous structure of the silicate and hydroxyl bonds. A series of experiments with quartz and opal are presented in Figure 8. First, we heated a (nonhydrous) quartz sample to 1000 °C in the dry N_2 gas stream in the TGA. After cooling back to room temperature, the dry N_2 gas flow was replaced with combined N_2 and water vapor stream (H_2O = 5000 ppm; $\delta^{18}O$ = −19‰; δD = −140‰). The sample was reheated in the presence of this wet gas stream. No change in δD is observed, but $\delta^{18}O$ begins to climb slowly between 600 and 1000 °C to reach a maximum of −14‰. The shift toward enriched values could be due to interactions of the H_2O with an enriched oxygen source. Possible sources include the following: the quartz sample (natural range +5−15‰), Al_2O_3 that makes up the crucible and furnace tube (+5−15‰)[33] or trace amounts of atmospheric O_2 in the gas stream (+23.5‰).[34]

The same experiment was then repeated with a biogenic silica sample in place of the quartz. The sample is a terrestrial diatomite of quaternary age from central Oregon[35] (local meteoric water $\delta^{18}O$ ~−13.5‰; mean annual temperature ~+8°C). The $\delta^{18}O$ of the nonhydrous oxygen of this sample is not precisely known but based on possible fractionation factors probably ranges between 20‰ and 28‰.

During the dehydroxylation of the sample from ~400 to 600 °C, $\delta^{18}O$ plateaus at about +7‰ and δD slowly trends to background values (the peak in $\delta^{18}O$ around 400°C is an example of organic contamination with an inert carrier gas and no catalyst). Upon reheating under a H_2O/N_2 mix atmosphere we again observe no shifts in the δD trace but a much larger shift in $\delta^{18}O$. The $\delta^{18}O$ begins to increase around 300 °C and reaches a maximum of +5‰ by 1000 °C. This shift is comparable to the change in $\delta^{18}O$ observed during dehydroxylation of the same sample.

DOI: 10.1021/acs.analchem.7b03136
Anal. Chem. 2018, 90, 752−759

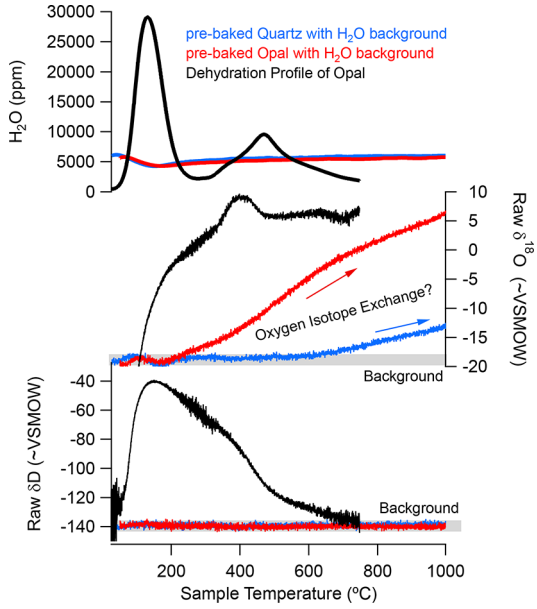

Figure 8. Possible oxygen isotope exchange. A series of experiments to demonstrate the potential of oxygen isotope exchange at high temperature. First, a sample of quartz was heated under dry N_2 to 1000 °C (not shown). After cooling to room temperature a stream of H_2O vapor (H_2O = 5000 ppm; $\delta^{18}O$ = −19‰; δD = −140‰ as indicated by gray horizontal bars) was added to the N_2 stream. The quartz sample was reheated to 1000 °C, and the H_2O, $\delta^{18}O$, and δD traces were monitored (blue line). The same experiment was repeated with an opal sample, first by heating the raw samples (black line) and then by imposing a water background over the now dehydrated samples (red line). Increase in the $\delta^{18}O$ trace during the water background experiments may indicate exchange between H_2O and an enriched source.

These experiments suggest that the system is free of any significant contamination or exchange with respect to hydrogen isotopes. Oxygen isotope measurements, however, could be significantly biased, possibly through exchange with isotopically enriched oxygen. This is not surprising given that the extraction system and the mineral samples are free of any nonhydrous hydrogen isotope sources, but nonhydrous oxygen is present in abundance. For example, a typical biogenic opal sample may hold about ∼10 wt % H_2O, ∼1 wt % OH, and ∼42 wt % nonhydrous oxygen. Overall, the results suggest that minerals that dehydroxylate at high temperature should be evaluated for possible oxygen isotope exchange.

CONCLUSIONS

We have demonstrated a new method for measuring the isotopic composition of multiple forms of bonded water in hydrous minerals. The method simultaneously provides $\delta^{18}O$ and δD data at precisions of 0.12‰ and 0.8‰, respectively. These precisions are comparable to those of previous methodologies for natural samples, if not a slight improvement (see Table 1 for comparison). However, the new method requires about 1 μL of water and is thus a slight compromise on sample size, in particular compared to online-IRMS methods capable of measurements of only 0.1 μL of water. Compared to offline differential thermal separation, the online-DTIA is significantly less labor intensive. The instrumental setup also requires much lower capital and consumables costs compared to methods utilizing gas-source mass spectrometers.

The primary advantage of the method is the ability to rapidly characterize the wt % and isotopic composition of multiple forms of bonded H_2O or bonded OH in a sample. By separating these different forms of water, factors that control the isotopic composition of the water species, such as isotopic fractionation during formation and postdepositional exchangeability, can now be studied. The same principle could also provide a way to separate water from different minerals in natural samples of mixed mineralogy.

The presence of organic matter, carbonate minerals, or exchangeable (nonhydrous) oxygen may effect the $\delta^{18}O$ measurement on minerals that undergo water loss at high temperature (∼>400°C). Minerals that undergo dehydration at relatively low temperature (e.g., gypsum, trona, nahcolite, and many other evaporite minerals) are likely free of these problems.

AUTHOR INFORMATION

Corresponding Author

*E-mail: tkb28@cam.ac.uk.

ORCID

T. K. Bauska: 0000-0003-1901-0367

Notes

The authors declare no competing financial interest.

ACKNOWLEDGMENTS

This research was supported by the ERC WIHM Project (#339694) to D.A.H. We thank James Rolfe and Ian Mather for technical assistance in the Godwin Laboratory.

REFERENCES

(1) Friedman, I.; Smith, R. L. *Geochim. Cosmochim. Acta* **1958**, *15*, 218−228.

Table 1. Method Precision Overview

	sample size		precision (‰,1σ sd)			
method	gypsum (mg)	H_2O (μL)	$\delta^{18}O$	δD	$\delta^{17}O$	ref
online DTIA	7	>1	0.12	0.8		this study
vacuum extraction - CRDS	200	40	0.13	0.5	0.07	Gazquez et al., 2015
online combustion OA-ICOS	2.00	0.40		3 to 4		Koehler and Wassenaar, 2012
TCEA-IRMS		0.1	0.2	2		Sharp et al., 2001
online reduction-IRMS		1.00×10^{-05}		1 to 2		Eiler and Kitchen, 2001
fluid inclusion CRDS		0.3 to 1.0	0.5	2		Arienzo et al., 2013
		>0.5	0.4	1.5		Affolter et al., 2014
		0.05 to 0.25	0.05 to 0.6	0.0 to 3.0		Uemura et al. 2016

DOI: 10.1021/acs.analchem.7b03136
Anal. Chem. 2018, 90, 752−759

(2) Gonfiantini, R.; Fontes, J. C. *Nature* **1963**, *200*, 644−646.
(3) Knauth, L. P.; Epstein, S. *Geochim. Cosmochim. Acta* **1976**, *40*, 1095−1108.
(4) Savin, S. M.; Epstein, S. *Geochim. Cosmochim. Acta* **1970**, *34*, 25−42.
(5) Savin, S. M.; Epstein, S. *Geochim. Cosmochim. Acta* **1970**, *34*, 43−63.
(6) O'Neil, J. R.; Kharaka, Y. K. *Geochim. Cosmochim. Acta* **1976**, *40*, 241−246.
(7) Suzuoki, T.; Epstein, S. *Geochim. Cosmochim. Acta* **1976**, *40*, 1229−1240.
(8) Yeh, H.-W.; Epstein, S. *Geochim. Cosmochim. Acta* **1978**, *42*, 140−143.
(9) Sheppard, S.; Gilg, H. *Clay Miner.* **1996**, *31*, 1−24.
(10) Matsuo, S.; Friedman, I.; Smith, G. I. *Geochim. Cosmochim. Acta* **1972**, *36*, 427−435.
(11) Hariya, Y.; Tsutsumi, M. *Contrib. Mineral. Petrol.* **1981**, *77*, 256−261.
(12) Knauth, L. P.; Epstein, S. *Am. Mineral.* **1982**, *67*, 510−520.
(13) Brand, W. A.; Tegtmeyer, A. R.; Hilkert, A. *Org. Geochem.* **1994**, *21*, 585−594.
(14) Sharp, Z. D.; Atudorei, V.; Durakiewicz, T. *Chem. Geol.* **2001**, *178*, 197−210.
(15) Eiler, J. M.; Kitchen, N. *Geochim. Cosmochim. Acta* **2001**, *65*, 4467−4479.
(16) Gázquez, F.; Mather, I.; Rolfe, J.; Evans, N. P.; Herwartz, D.; Staubwasser, M.; Hodell, D. A. *Rapid Commun. Mass Spectrom.* **2015**, *29*, 1997−2006.
(17) Arienzo, M. M.; Swart, P. K.; Vonhof, H. B. *Rapid Commun. Mass Spectrom.* **2013**, *27*, 2616−2624.
(18) Affolter, S.; Fleitmann, D.; Leuenberger, M. *Clim. Past* **2014**, *10*, 1291−1304.
(19) Uemura, R.; Nakamoto, M.; Asami, R.; Mishima, S.; Gibo, M.; Masaka, K.; Jin-Ping, C.; Wu, C.-C.; Chang, Y.-W.; Shen, C.-C. *Geochim. Cosmochim. Acta* **2016**, *172*, 159−176.
(20) Koehler, G.; Wassenaar, L. I. *Anal. Chem.* **2012**, *84*, 3640−3645.
(21) Földvári, M. *Handbook of Thermogravimetric System of Minerals and Its Use in Geological Practice*; Occasional Papers of the Geological Institute of Hungary; Geological Institute of Hungary: Budapest, 2011; Vol. *213*.
(22) Hodell, D. A.; Turchyn, A. V.; Wiseman, C. J.; Escobar, J.; Curtis, J. H.; Brenner, M.; Gilli, A.; Mueller, A. D.; Anselmetti, F.; Ariztegui, D.; Brown, E. T. *Geochim. Cosmochim. Acta* **2012**, *77*, 352−368.
(23) Aemisegger, F.; Sturm, P.; Graf, P.; Sodemann, H.; Pfahl, S.; Knohl, A.; Wernli, H. *Atmos. Meas. Tech.* **2012**, *5*, 1491−1511.
(24) Steen-Larsen, H. C.; Johnsen, S. J.; Masson-Delmotte, V.; Stenni, B.; Risi, C.; Sodemann, H.; Balslev-Clausen, D.; Blunier, T.; Dahl-Jensen, D.; Ellehøj, M. D.; Falourd, S.; Grindsted, A.; Gkinis, V.; Jouzel, J.; Popp, T.; Sheldon, S.; Simonsen, S. B.; Sjolte, J.; Steffensen, J. P.; Sperlich, P.; Sveinbjörnsdóttir, A. E.; Vinther, B. M.; White, J. W. C. *Atmos. Chem. Phys.* **2013**, *13*, 4815−4828.
(25) Sheppard, S. M. F. *J. Geol. Soc.* **1977**, *133*, 573.
(26) West, A. G.; Goldsmith, G. R.; Brooks, P. D.; Dawson, T. E. *Rapid Commun. Mass Spectrom.* **2010**, *24*, 1948−1954.
(27) Gemery, P. A.; Trolier, M.; White, J. W. C. *J. Geophys. Res. Atmospheres* **1996**, *101*, 14415−14420.
(28) Bottinga, Y. *J. Phys. Chem.* **1968**, *72*, 800−808.
(29) Truesdell, A. H. *Earth Planet. Sci. Lett.* **1974**, *23*, 387−396.
(30) McManus, J. B.; Nelson, D. D.; Zahniser, M. S. *Opt. Express* **2015**, *23*, 6569−6586.
(31) McCrea, J. M. *J. Chem. Phys.* **1950**, *18*, 849−857.
(32) Sharma, T.; Clayton, R. N. *Geochim. Cosmochim. Acta* **1965**, *29*, 1347−1353.
(33) Lawrence, J. R.; Taylor, H. P. *Geochim. Cosmochim. Acta* **1971**, *35*, 993−1003.
(34) Kroopnick, P.; Craig, H. *Science* **1972**, *175*, 54.
(35) VanLandingham, S. L. *Micropaleontology* **1990**, *36*, 182−196.

DOI: 10.1021/acs.analchem.7b03136
Anal. Chem. 2018, 90, 752−759